Precision of the Jaw Tracking System JAWS-3D

Ruggero L. Airoldi, Dr med dent
Assistant

Luigi M. Gallo, Dr Sc Tech
Senior Research Associate

Sandro Palla, Dr med dent
Professor and Chairman

Department of Masticatory Disorders
and Complete Dentures
Dental School
University of Zurich
CH-8028 Zurich
Switzerland

Correspondence to Dr Gallo

The purpose of this study was to measure, under laboratory conditions, the noise level of the optoelectronic jaw-tracking system JAWS-3D, which records the movement of the whole mandible from extraorally placed landmarks. Also, an assessment was made of its accuracy in measuring positions, angles, and velocities. The results showed that the accuracy of JAWS-3D decreased when the distance between the recorded point and the extraoral landmarks increased. The path of a point near to the landmarks was estimated with an error of 0.11%, whereas the error increased to 1.33% when the point was far from the landmarks. The maximum error in angle computation was 0.7 degrees. The velocities calculated by JAWS-3D corresponded closely to the actual ones: mean error of 3 mm/s for velocities up to 80 mm/s. Thereafter, the error increased to reach 26 mm/s at a speed of 210 mm/s.
J OROFACIAL PAIN 1994;8:155–164.

Several electronic systems for recording jaw movements have been developed in the past, the most well known being: the Case Gnathic Replicator[1–5]; the Kinesiograph[6–10]; the Sirognathograph[10–14]; the Selspot system[15–17]; the Axiograph[18–21]; and the String-LR-Recorder.[22] Several other systems have also been described.[23–33] The difficulty in constructing a system that meets all the requirements necessary to record jaw function may well explain why so many jaw tracking devices have been developed. Such a device should not be invasive, and it should not interfere with jaw and soft tissue function or restrict head movements. It should be simple to use, and, finally, it should record the movement of the whole mandible, not only of a single point. With this in mind, a noninvasive, optoelectronic system, called JAWS-3D, has been developed.[34–41] This system describes three-dimensionally and in real time the movement of the whole mandible. Head movements are not restricted and lip function is minimally disturbed.

Despite the claim that jaw tracking devices have to be very precise and accurate, few papers have analyzed these issues. Error measurements have been investigated for the Kinesiograph,[6–9] the Selspot system,[15,16] and the Sirognathograph.[42] These devices record the movement of a single mandibular point. Thus, their measurement error depends upon the limitations of the hardware itself, eg, the nonlinearity of the magnetic field, the resolution degree of the sensors, the detector's noise, and the system's sampling rate. In contrast, JAWS-3D records the movement of the whole mandible as a rigid body, with 6 degrees of freedom, by means of extraorally placed landmarks. The movement of a mandibular point is calculated by geometric reconstruction from the coordinates of the extraoral landmarks. This computation is an additional source of error; therefore, an analysis of the performance of JAWS-3D requires not only a determination of the precision and accuracy

with which a movement is recorded on the landmarks but also knowledge of how precisely the movement of the mandibular point can be estimated. This error depends also upon the distance between the recording sites and the mandibular point.[43] For instance, the error in measuring the length of a linear trajectory with the first version of JAWS-3D varied between 0.64% and 2.93% and the error in recording its steepness ranged between 0.62% and 6.45% when the distance between selected point and landmarks increased from 87 mm to 164 mm.[44]

The aim of this study was to continue Velkoborsky's investigation[44] by measuring the noise and the precision with which a new version of JAWS-3D can measure length, angles, and velocities under laboratory conditions. This new version of the system has improved landmarks with stronger light sources and more precise software for coordinates reconstruction and data analysis.

Material and Methods

The JAWS-3D System

This optoelectronic system consists of three charge-coupled device (CCD) linear cameras that record the position of six light-emitting diodes (LED) connected to the mandible and the maxilla. These are mounted on two triangular target frames attached to the upper and the lower dental arches by means of custom-made metal splints (Fig 1).[40] A specially developed interface board in an IBM AT compatible personal computer drives the LEDs, generates the cameras' timing signals, and preprocesses the signals generated by the cameras. Each camera contains a cylindrical lens, a one-dimensional CCD optosensor array, and electronic circuitry. The one-dimensional CCD optosensor arrays contained in the cameras are mounted along the axes of an orthogonal coordinate system. By means of the cylindrical lens, each camera records one coordinate of the position of the LEDs that are sequentially fired by the interface. A maximum detector circuitry determines the location on each CCD sensor of the cell most illuminated by the LED currently fired. The spatial coordinates of the LEDs are computed from the locations of the spots on the sensors as well as from the fixed geometry and optical properties of the system. The system allows linear recordings of the LEDs' positions within a view field of a cube with a side of 140 mm.[33] The LED coordinates are reconstructed by a local 16-bit TMS9995 microprocessor in less than 1 ms.

Each of the lightweight target frames (4.8 g wires included) defines a jaw-related coordinates system (Fig 2). JAWS-3D records the head motion from the position of the LEDs of the upper frame and the combined motion of head and mandible from the position of the LEDs of the lower frame. Knowing the coordinates of a mandibular point in the lower target coordinate system, the computer can calculate the movement of this point in the head-related coordinates system. The coordinates of the mandibular point to the lower target frame are recorded directly by the system by means of specially designed, calibrated intraoral and extraoral pointers bearing one or three LEDs. This process is called preselection, and the chosen point is called the preselected point. The computation of the coordinates of a preselected point is done in less than 12 ms. The system's sampling rate is 70 Hz.[35,38] Details are further discussed elsewhere.[35,38,40]

Noise and Length Estimation

The system's noise was analyzed under static and dynamic conditions, ie, with both target frames immobile and with both target frames moving. The setting for the dynamic condition is described below. To test the noise and the precision of JAWS-3D, a device to hold the reference target frames and simulate a translatory movement had to be constructed (Fig 3). This device consisted of a metal plate with two posts. The left post was connected by means of a high-precision cardanic joint to a metal beam, whose right end (right joint) was free to slide in an anteroposterior direction on an inclined, sharp metal surface that was 18.8 mm long. To preselect the right joint center, a cone-shaped hole with its apex located exactly in the center of the metal beam was drilled at 10 mm from its right end, ie, at the intersection between the beam and the edge of the inclined plane (Fig 4). The lower target frames were fixed bilaterally by means of a cross-bar to an L-shaped bar attached to the moving beam. The upper frames were fixed to the vertical posts so that the Z-axis was vertical, the X-axis was horizontal, and the Y-axis was parallel to the metal beam. No special attempt was made to position the lower target frame parallel to the upper one.

To analyze the system's noise under static conditions, the positions of the LED with coordinates 0/0/0 (lowest LED) and the right joint center were computed from the signals recorded with the device immobile for 10 seconds. The CCD cameras were positioned first on the right and then on the

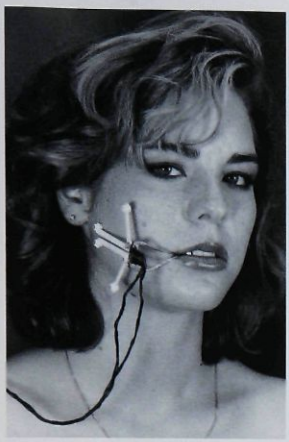

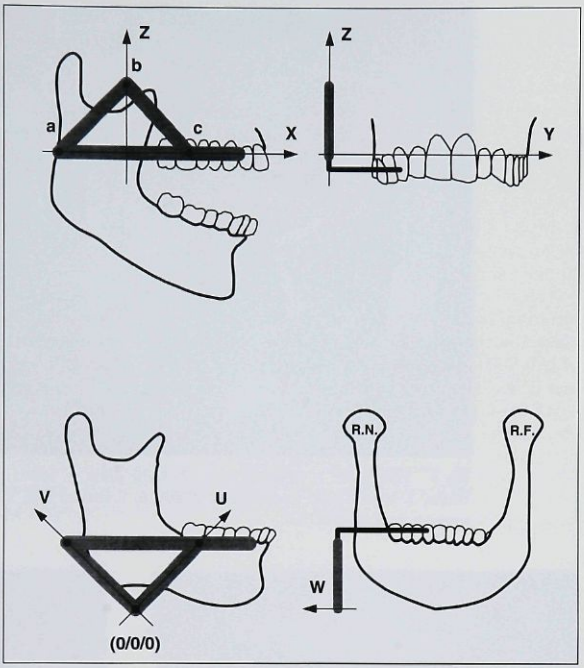

Fig 1 *(Above)* Patient with the reference triangles fixed to the maxilla and mandible.

Fig 2 *(Right)* Coordinates of the upper (x, y, z) and lower (u, v, w) reference triangle. (RN = reference near joint; RF = reference far joint; 0/0/0 = coordinates of the lowest LED.)

left side of the device at randomly chosen distances of 253 (D1), 274 (D2), 277 (D3), and 305 mm (D4) from the target frames. Therefore, the position of the LED was computed four times and that of the joint center eight times. The position of this last point was preselected both with the frame on the same, right side ("reference near") as well as on the opposite, left side ("reference far") (Fig 5), the u, v, and w coordinates being 12, 96, and –17 mm for the reference near setting and 24, 113, and 141 for the reference far setting. Therefore, the terms reference near and reference far refer to the position of the joint center relative to the target frames. For instance, the joint center was reference near when its position was computed from the information parameters of the target frames mounted on the same side and reference far when its position was calculated from the parameters of the frames placed on the opposite left side. Recordings with the cameras on both sides allowed evaluation of the effect of the distance between target frames and preselected point on the noise level. The noise was defined as the standard deviation of the positions of the preselected point over the 10 seconds.

To measure the precision with which JAWS-3D calculates the length of a trajectory, the metal beam was moved 10 times along the inclined plane, from posterior to anterior (Fig 4). Measurements were performed first with the CCD cameras on the right side and thereafter on the left side. Again, this allowed calculation of the measurement precision as a function of the distance target frames–preselected point. After each movement, the computed trajectory was displayed on the computer screen, the beginning and ending were marked by means of the cursor, and the trajectory length was calculated according to the formula:

$$L = \sqrt{x^2 + y^2 + z^2}$$

Means and standard deviations were computed for both reference near and reference far measurements.

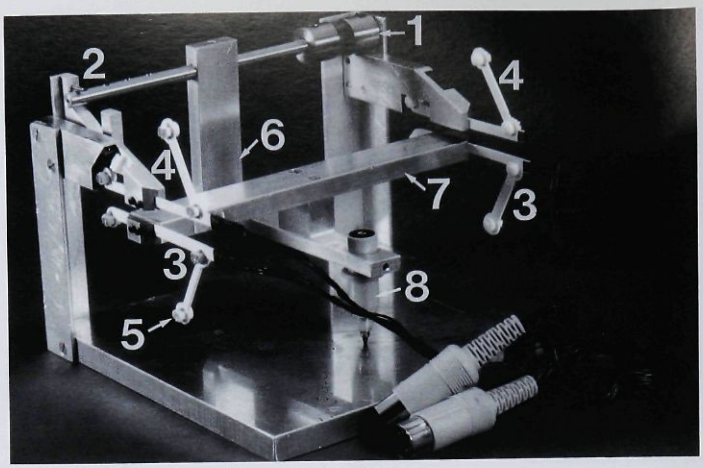

Fig 3 Simulator: 1. cardanic joint, 2. right joint, 3. lower target frame, 4. upper target frame, 5. lowest LED (coordinates 0/0/0), 6. L-shaped bar, 7. cross bar, 8. anterior pin to support the L-shaped bar.

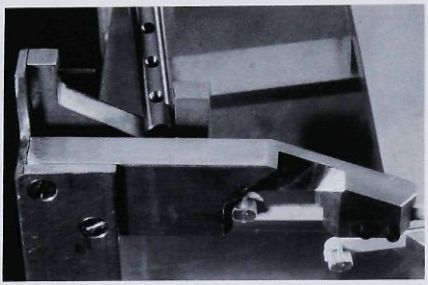

Fig 4 Metal beam with cone-shaped holes to preselect the right joint center.

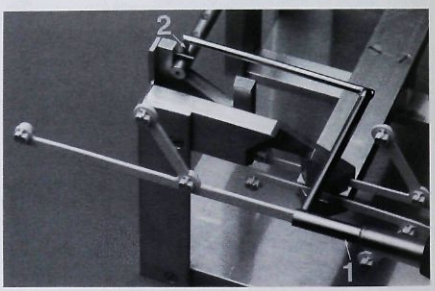

Fig 5 Preselection of the right joint center by means of a pointer (1) with fixed geometry. The pointer's tip (2) is inserted in the cone-shaped hole of the metal beam. From the coordinates of the pointer's triangle relative to those of the lower target frame, the computer calculates the position of the pointer's tip.

Angle Measurement

For this experiment, another device had to be constructed (Fig 6). A goniometer was attached to a plastic panel by means of a hinge-axis passing trough its center. One of the target frames was attached to the goniometer, the other one to the plastic panel. In the reference position (angle 0 degrees), the V-axis of the goniometer's target frame was parallel to the X-axis of the panel's target frame. After placing the panel parallel to the XZ-plane of the CCD cameras, the positions of the V-axis LEDs were preselected. Thereafter, the goniometer was rotated from 0 to 90 degrees in steps of 5 degrees. For each angle, the LED's position was recorded during 5 s. From the mean position of the LEDs over the 5 s, the computer calculated the angle between the V- and X-axes of the target frames.

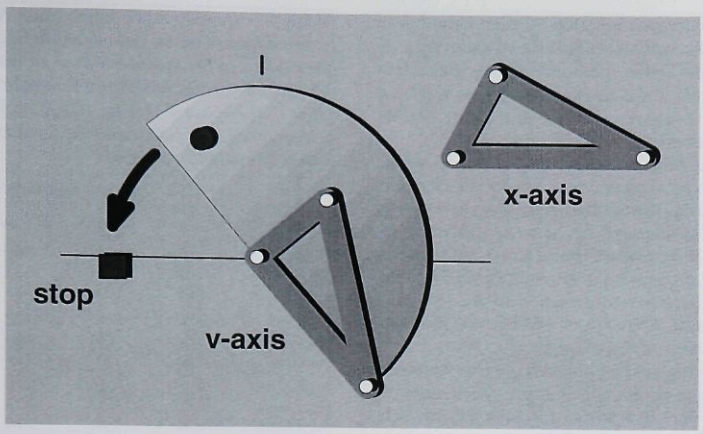

Fig 6 Graphic representation of the device for angle measurement. The goniometer could rotate around the hinge-axis. One of the target frames was attached to the goniometer, the other one to the panel. The computer calculated the angle between the V- and X-axes of the target frames, which was varied between 0 to 90 degrees in steps of 5 degrees.

Velocity Measurement

These measurements were performed by means of another device that generated linear movements with sinusoidal velocity (Fig 7). The device consisted of an aluminum disc driven by a direct current motor and a horizontally moving sled. The sled's movement, which occurred parallel to the system's X-axis, was achieved by connecting its vertical slotted bar to the disc by means of a shaft fixed in the radially oriented slot of the disc. By varying the position of the shaft in the radial slot and by applying different DC voltages to the motor, the amplitude and velocity of the sled's movement could be changed. A code wheel fixed to the disc's axis and an incremental optical encoder allowed measurement of the disc's rotatory frequency and computation of the maximum velocity (in mm/s) reached by the sled. To record velocity, one target frame was mounted on the pole above the disc and the other one on the sled's vertical bar. To analyze the noise under dynamic conditions, both target frames were mounted on the sled's vertical bar, so that they moved synchronously. For this last test, the computer calculated the standard deviation of the instantaneous positions of the lowest LED (coordinates 0/0/0).

A total of 23 sets of velocity measurements were performed for both tests by incrementing the sled's maximum velocity between 10 and 230 mm/s in steps of 10 mm/s. As the JAWS-3D system can record movements for a maximum of 26 s at a time, a minimum of 30 up to a maximum of 52 cycles per velocity setting were recorded. The instantaneous velocities of the lowest LED (coordinates 0/0/0) of the sled's target frame were calculated by dividing the distance between consecutive points by the sample time of 14 ms. As the velocity signal is more strongly affected by noise than the position signal, a digital finite impulse response, low-pass filter was used to suppress the noise. An

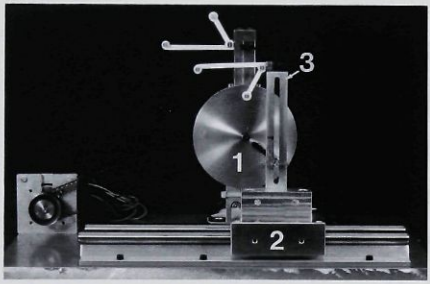

Fig 7 Generator of linear movements with sinusoidal velocity. 1. aluminum disc, 2. sled, 3. vertical slotted bar. (Setting for velocity measurement.)

optimum linear combination of nine values was chosen, with coefficients calculated according to the Parks-McClellan method.[45] A pass band frequency of 5 Hz and a ripple of 0.1 dB, as well as a stop band frequency of 20 Hz and ripple of 100 dB, were selected.

To analyze how the noise is dependent on velocity, the filtered x component of the velocity was subtracted from the unfiltered one for each velocity setting. The standard deviation of this resulting signal was the noise of the velocity signal. The noise of the system under dynamic conditions was defined as the standard deviation of the instantaneous positions of the lowest LED. It was also calculated for every tested velocity.

To study the correspondence degree between actual and measured velocities the mean velocity maximums were determined for each velocity setting and differences were calculated.

Results

Noise

The noise level recorded under static conditions at the lowest LED varied between 0.01 and 0.04 mm. That of the center of the right joint varied between 0.02 and 0.04 mm for reference near measurements and between 0.12 and 0.34 mm for reference far measurements (Table 1). Under dynamic conditions, the mean and standard deviation of the noise level for the 22 tested velocities was 0.17 ± 0.05 mm (range 0.05 to 0.35 mm).

Length of Trajectories

The error in computing the length of the trajectory (actual length 18.8 mm) was greater when the preselected point was on the reference far side than when it was on the reference near side. On the average, the calculated length of the trajectory was 18.78 ± 0.07 mm (relative error 0.11%) for the reference near side and 18.55 ± 0.23 mm (relative error 1.33%) for the reference far side (Table 2).

Angles Measurement

The calculated values were very close to the actual ones, the difference varying between 0.1 and 0.7 degrees (mean and SD = 0.37 ± 0.22 degrees). The correlation coefficient between actual and calculated values was $r^2 = 1.00$ (Fig 8).

Table 1 System's Static Noise (mm) Along the x, y, and z Coordinates, Calculated as Standard Deviations of the Position Values of the Lowest LED (Coordinates 0/0/0) and the Right Simulator Joint (RJ) Recorded During 10 s With Landmarks Mounted on the Ipsilateral Side (ipsi) and on the Contralateral Side (contra)

	Recording distance			
Position	253 mm	274 mm	277 mm	305 mm
LED_x	0.02	0.02	0.01	0.01
LED_y	0.03	0.03	0.03	0.02
LED_z	0.02	0.04	0.03	0.03
RJ_x (ipsi)	0.02	0.02	0.02	0.02
RJ_y (ipsi)	0.04	0.04	0.04	0.04
RJ_z (ipsi)	0.03	0.04	0.03	0.03
RJ_x (contra)	0.14	0.15	0.15	0.18
RJ_y (contra)	0.12	0.12	0.12	0.14
RJ_z (contra)	0.30	0.31	0.30	0.34

Table 2 Mean Length ± SD and Relative Error of Right Simulator Joint Trajectories Recorded With Reference Triangles Mounted on Ipsilateral and Contralateral Side

	Triangles on	
	Ipsilateral side	Contralateral side
Length (mm)	18.78 ± 0.07	18.55 ± 0.23
Relative error (%)	0.11	1.33

Actual trajectory length 18.8 mm.

Velocity Measurement

The noise values for each selected maximum velocity were normally distributed with mean values smaller than 0.005 mm/s. Their standard deviations increased with increasing velocity, the values ranging between 3.97 mm/s at the speed of 20 mm/s and 19.03 mm/s at the speed of 210 mm/s (Fig 9).

A good correspondence between the velocity maximums of the actual and calculated velocities was found for velocities up to 80 mm/s, with a mean discrepancy of 3 mm/s. For velocities above 80 mm/s, this discrepancy increased to 26 mm/s at the velocity of 230 mm/s (Fig 10).

Discussion

This study showed that the measurement error increased as the distance between the selected point and the LEDs increased, which confirmed

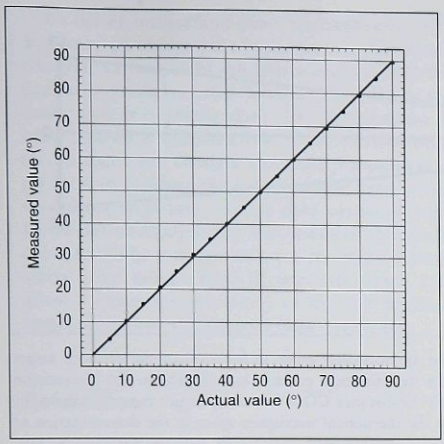

Fig 8 Relationship between measured angles and actual values. The solid line represents the linear regression (r^2 = 1.00) and each dot represents the angle computed from the mean position of the LEDs over 5 s.

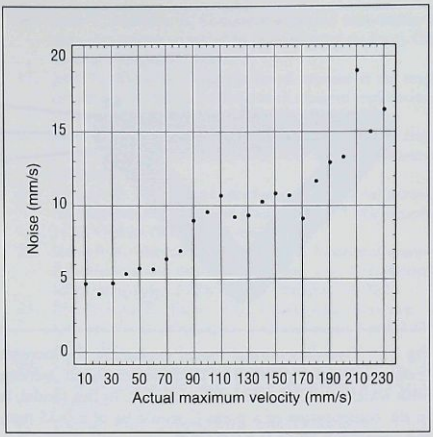

Fig 9 Relationship between the recorded noise in mm/s vs maximum velocity. The sudden noise increase around 80 to 90 mm/s was most likely caused by an increase in the amplitude of the vibration of the triangles as well as by mechanical resonances.

the results by Velkoborsky.[44] Comparison of these results with those in the present study indicates an improvement in the performance of the new system. The position of the lowest LED was recorded in the previous study with a noise level of 0.09 mm, which was more than twice as large as in the present study (0.04 mm). Also, the error in the computation of the length of a trajectory was larger in the Velkoborsky study, in which it varied between 0.64% (reference near) and 2.93% (reference far). The corresponding values in the present study were 0.11% and 1.33%. The distance-dependent increase of the measurement error is mainly due to the imprecision with which the LED position is recorded.[43] The CCD sensor registers the LED position by detecting the peak value of the light signal emitted. As this has a bell-shaped curve, there is an uncertainty in the reconstruction of the preselected point. This phenomenon is explained in a simplified, two-dimensional manner in Fig 11. In this model, in which the distance $\overline{CO}$ is five times larger than $\overline{AO}$, the error in the computation of point C would be ± 0.35 mm, being the theoretical maximum error in the determination of the position of an LED ± 0.07 mm.[38]

The error in the calculation of the length of a trajectory increased from 0.11% for reference near

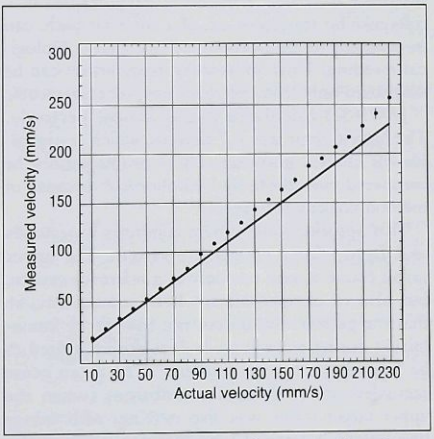

Fig 10 Relationship between the measured maximum velocities and the actual maximum velocities. Each dot represents the mean value of the measured maximum velocities. The standard deviations are so small that their representation mostly falls within the dot size. Velocities up to 80 mm/s were measured with quite good precision, the mean discrepancy being of 3 mm/s. The measurement error increased up to 26 mm/s for a velocity of 230 mm/s.

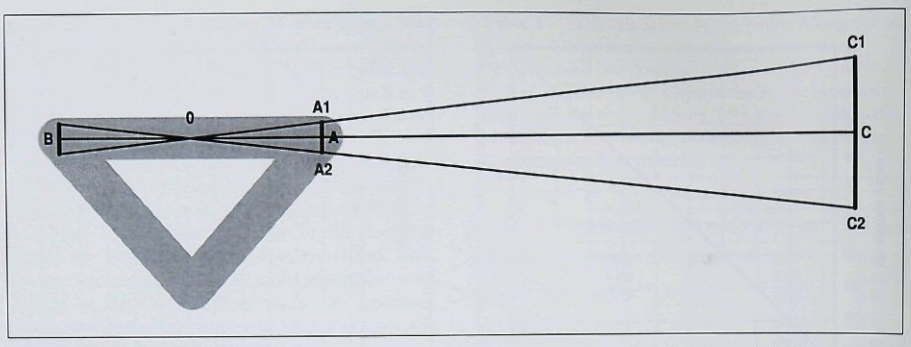

Fig 11 Two-dimensional model explaining the increase of the measurement error as function of the distance target frame-preselected point. The distance-dependent increase of the measurement error is mainly due to the imprecision with which the LED position is recorded. In this model, in which the distance $\overline{CO}$ is five times larger than $\overline{AO}$, the error in the computation of a point C would be of ± 0.35 mm, being the theoretical maximum error in the determination of the position of an LED ± 0.07 mm.

to 1.33% for reference far measurements. From a clinical standpoint, the larger error is acceptable. On the other hand as the noise increases with the distance target frame–preselected point, a reference far trajectory will always be less smooth than a reference near one. Therefore, irregularities in a reference far trajectory, eg, of a condylar path, can be inherent to the method and not have a biological meaning. Thus, movement irregularities can be diagnosed only from reference near measurements.

JAWS-3D calculated angles almost perfectly. The largest error was 0.7 degrees, which is negligible for clinical purposes. These results cannot be compared with those by Velkoborsky[44] because of methodological differences.

This optoelectronic system computes trajectories in a head-related coordinate system. The upper target frame is used not only as a reference system, but also to compensate for head movements, so that the patient's head does not have to be immobilized during recordings. It does not even need to be leaned against the headrest. The mean noise recorded under dynamic conditions (when the upper target frame was also moving, with velocities varying between 10 mm/s and 230 mm/s) was 0.17 mm. Thus, movements are well compensated, confirming that the patient's head does not have to be immobilized when recording jaw movements on the reference near side.

Velocities up to 80 mm/s were measured with quite good precision, the mean discrepancy being 3 mm/s. The measurement error increased to 26 mm/s for a velocity of 230 mm/s. This was also the case for the velocity noise. This phenomenon is partially due to the sequential firing of the LEDs, which makes it impossible to record simultaneously the position of all diodes. A noise level of 3.97 mm/s for an actual velocity of 20 mm/s may appear as disproportionate. However, the quantization error itself produces a noise in the velocity signal of up to 5 mm/s, being the theoretical resolution of the system 0.07 mm and the time resolution 14 ms (0.07 mm/14 ms = 5 mm/s). The sudden noise increase around 80 to 90 mm/s was most likely caused by an increase in the amplitude of the vibration of the triangles.

Comparison of our data with those of other recording systems is impossible because accuracy data were reported only for devices that record the movement of a single mandibular point.[6–9,15,16] For the other systems recording the movement of the whole mandible, only the precision degree at the sensor side was reported.[5]

The small error of JAWS-3D in recording reference near mandibular points together with its very low invasiveness degree warrants for its use in clinical research.[40,46–50] However a possible limiting factor of the system is the sampling frequency of 70 Hz, which is given by the LEDs' switching time and by the duration of the computation of the coordinates of the preselected point. Thus, very quick events happening in a 14-ms time window between two sample times might be lost. Nevertheless the optimum sampling frequency for jaw movement recording with 6 degrees of freedom has yet to be defined.

To better understand joint biomechanics, it is necessary to analyze the movement of the whole condylar surface within the fossa and not only the path of a condylar point without reference to the fossa, as it is normally done. The introduction of MRI allows a noninvasive, three-dimensional reconstruction of condyle and fossa. Research is in progress to combine three-dimensional joint reconstructions with jaw motion data obtained with JAWS-3D to analyze the movement of the whole condyle.[51] The analysis of how the three-dimensional joint space varies during movements may allow a better understanding of the disc function under normal as well as pathologic conditions.

References

1. Cannon DC, Reswick JB, Messerman T. Instrumentation for the investigation of mandibular movements. Eng Design Centre Rep. EDC 4-1964–8.
2. Gibbs CH, Messerman T. The Case gnathic replicator for the investigation of mandibular movements. Eng Design Centre Rep. EDC 4-1966–14.
3. Messerman T. A means for studying mandibular movements. J Prosthet Dent 1967;17:36–43.
4. Messerman T, Reswick JB, Gibbs C. Investigation of functional mandibular movements. Dent Clin North Am 1969;13:629–642.
5. Gibbs CH, Messerman T, Reswick JB, Derda HJ. Functional movements of the mandible. J Prosthet Dent 1971;26:604–620.
6. Jankelson B, Swain CW, Crane PF, Radke JC. Kinesiometric instrumentation: A new technology. J Am Dent Assoc 1975;90:834–840.
7. Hannam AG, Scott JD, DeCou RE. A computer-based system for the simultaneous measurement of muscle activity and jaw movement during mastication in man. Archs Oral Biol 1977;22:17–23.
8. Hannam AG, DeCou RE, Scott JD, Wood WW. The kinesiographic measurement of jaw displacement. J Prosthet Dent 1980;44:88–93.
9. Jankelson B. Measurement accuracy of the mandibular kinesiograph—A computerized study. J Prosthet Dent 1980;44:656–666.
10. Michler L, Bakke M, Moeller E. Graphic assessment of natural mandibular movements. J Craniomandib Disord Facial Oral Pain 1987;1:97–114.
11. Lewin A, Van Rensburg LB, Lemmer J. A method of recording the movement of a point on the jaws. J Dent Assoc S Afr 1974;29:395–397.
12. Lemmer J, Lewin A, Van Rensburg LB. The measurement of jaw movement. Part I. J Prosthet Dent 1976;36: 211–218.
13. Lewin A, Lemmer J, Van Rensburg LB. The measurement of jaw movement. Part II. J Prosthet Dent 1976;36: 312–318.
14. Lewin A, Nickel B. The full description of jaw movement. J Dent Assoc S Afr 1978;33:261–267.
15. Karlsson S. Recording of mandibular movements by intraorally placed light emitting diodes. Acta Odont Scand 1977;35:111–117.
16. Jemt T, Karlsson S. Computer-analysed movements in three dimensions recorded by light-emitting diodes. J Oral Rehabil 1982;9:317–326.
17. Jemt T, Olsson K. Computer-based analysis of the single chewing cycle during mastication in repeated registrations. J Prosthet Dent 1984;52:437–443.
18. Slavicek R. Axiographie. In: W Druecke, B Klemt (eds). Kiefergelenk und Okklusion. Berlin: Quintessenz, 1980:229–245.
19. Slavicek R. Clinical and instrumental functional analysis for diagnosis and treatment planning. Part 5. Axiography. J Clin Orthod 1988;22:656–667.
20. Slavicek R. Clinical and instrumental functional analysis for diagnosis and treatment planning. Part 7. Computer-aided axiography. J Clin Orthod 1988;22:776–787.
21. Piehslinger E, Celar AG, Celar RM, Slavicek R. Computerized axiography. J Craniomand Pract 1991; 9:344–355.
22. Klett R. Elektronisches Registrierverfahren fur die Kiefergelenksdiagnostik. Dtsch Zahnärztl Z 1982;37: 991–998.
23. Gillings BRD. Photoelectric mandibulography: A technique for studying jaw movements. J Prosthet Dent 1967;17:109–121.
24. Koerber KH. Elektronische Registrierung der Unterkieferbewegungen im normalen und okklusionsgestorten Gebiss. Dtsch Zahnärztl Z 1971;26:167–176.
25. Heners M. Ein elektronisches Verfahren zur Registrierung von sagittalen Grenzbewegungen des Unterkiefers. Dtsch Zahnärztl Z 1973;28:532–540.
26. Honee GLJM, Meijer AA. A method for jaw movement registration. J Oral Rehabil 1974;1:217–221.
27. Grassl H. Opto-electronic monitoring of mandibular movements [abstract]. J Dent Res 1978;57(special issue).
28. Koerber E, Lueckenbach A. Dreidimensionale Darstellung der Bewegung einzelner Punkte eines Kiefermodelles im Artikulator. Dtsch Zahnärztl Z 1981;36:462–466.
29. Koerber E, Lueckenbach A. Beitrag zur Registrierung der räumlichen Bewegung des Unterkieferinzisalpunktes und der Kondylen. Quintessenz 1982;33:1915–1925.
30. Hobo S, Mochizuki S. A kinematic investigation of mandibular border movements by means of an electronic measuring system. Part I: Development of the measuring system. J Prosthet Dent 1983;50:368–373.
31. Fischer-Brandies H, Burckhardt R, Kluge G. Reproduzierbarkeit der Messergebnisse der optoelektronischen Achsiographie mit dem Stereognathographen V. Z Stomatol 1990;87:359–367.
32. Maurice K, Leberl F, Curry S, Kober W. Real-time close-range 3D motion measurements for dental medicine. SPIE 1990;1395:366–373.
33. Siegler S, Hayes R, Nicolella D, Fielding A. A technique to investigate the three-dimensional kinesiology of the human temporomandibular joint. J Prosthet Dent 1991;65:833–839.
34. Mesqui F. Optoelectronic (SELSPOT) mandibular movement measurement and description with 6 degrees of freedom of the human jaw motion. Proceedings of the 4th Meeting of the European Society of Biomechanics: Davos, Switzerland (1984).
35. Mesqui F, Kaeser F, Fischer P. Real-time noninvasive recording and three-dimensional display of the functional movements of an arbitrary mandible point. Proc SPIE 1985;602:77.
36. Mesqui F, Palla S. Non invasive optoelectronic recording of jaw movement [abstract]. J Dent Res 1985;64(special issue).

37. Palla S. Neue Erkentnisse und Methoden in der Diagnostik der Funktionsstörungen des Kausystems. Schweiz Mschr Zahnmed 1986;96:1329–1351.
38. Mesqui F, Kaeser F, Fischer P. On-line three-dimensional light spot tracker and its application to clinical dentistry. Int Arch Photogrammetry Rem Sens 1986;26: 310–317.
39. Mesqui F, Kaeser F, Fischer P, Palla S. Accuracy and reproducibility of an Universal Jaw Motion Recorder [abstract]. J Dent Res 1987;65(special issue).
40. Merlini L, Palla S. The relationship between condylar rotation and anterior translation in healthy and clicking temporomandibular joints. Schweiz Mschr Zahnmed 1988;98:1191–1199.
41. Airoldi RL, Gallo LM, Palla S. Assessment of precision of the JAWS-3D jaw tracking system [abstract]. J Dent Res 1992;71(special issue).
42. Balki MK, Tallents RH. Error analysis of a magnetic jaw-tracking device. J Craniomandib Disord Facial Oral Pain 1991;5:51–56.
43. Woltring HJ, Huiskes R, DeLange A, Veldpaus FE. Finite centroid and helical axis estimation from noisy landmark measurements in the study of human joint kinematics. J Biomech 1985;18:379–389.
44. Velkoborsky V. Möglichkeiten und Grenzen eines an der Universität Zürich entwickelten optoelektronischen Gerates für die Registrierung von Unterkieferbewegungen: Jaws-3D [thesis]. University of Zurich, 1989.
45. Loy NJ. An Engineer's Guide to FIR Digital Filters. Englewood Cliffs, NJ, Prentice Hall, 1988:90–99.
46. Ernst B. Condylar path and translatory velocity changes in clicking temporomandibular joints [thesis]. University of Zurich, 1988.
47. Salaorni C, Palla S. Condylar rotation and anterior translation in healthy human temporomandibular joints. Schweiz Mschr Zahnmed 1994;104:415–422.
48. Rohrer F, Palla S, Engelke W. Condylar movements in clicking joints before and after arthrography. J Oral Rehabil 1991;18:111–123.
49. Witt E. Variations in condylar velocity during opening and closing in healthy human temporomandibular joints [thesis]. University of Zurich, 1991.
50. Witt E, Palla S. Condylar velocity during opening and closing in healthy human [abstract]. J Dent Res 1992;71(special issue).
51. Krebs M, Gallo LM, Airoldi RL, Palla S. Animation of MR-images of the TMJ by opto-electronically recorded movements [abstract]. J Dent Res 1993;72(special issue).

Resumen

Precisión del sistema de rastreo mandibular JAWS-3D

El propósito de este estudio fue el de medir en un laboratorio, el nivel del sonido del sistema de rastreo mandibular optoelectrónico JAWS-3D, el cual registra el movimiento de toda la mandíbula desde guías de referencia colocadas extraoralmente. También, se efectuó una evaluación de su precisión para medir posiciones, ángulos y velocidades. Los resultados demuestraron que la precisión del sistema JAWS-3D disminuyó cuando la distancia entre el punto registrado y el punto de referencia extraoral aumentó. El curso de un punto cercano a las guías de referencia fue estimado con un error del 0.11%, mientras que el error aumentó a 1.33% cuando el punto estaba lejos de éstas. El error máximo en el cómputo del ángulo fue de 0.7%. Las velocidades calculadas por el sistema JAWS-3D correspondieron fielmente a las efectivas: un error (media) de 3 mm/s para las velocidades hasta de 80 mm/s. Subsecuentemente, el error aumentó hasta alcanzar 26 mm/s a una velocidad de 210 mm/s.

Zusammenfassung

Genauigkeit des Systems JAWS-3D Zur Aufzeichung von Unterkeiferbewegungen

Das opto-elektronische System JAWS-3D berechnet die Bewegung des ganzen Unterkiefers aus der Lage von extraoral plazierten Referenzen. Ziel dieser Studie war die Messung im Labor von Messrauschen und -genauigkeit des Systems bei der Berechnung von Positionen, Winkeln und Geschwindigkeiten. Die Resultate zeigen, dass die Genauigkeit von JAWS-3D abnimmt, wenn die Distanz zwischen dem untersuchten Punkt und den Referenzen zunimmt. Tatsächlich war der Fehler bei der Aufzeichnung von Trajektorien 0.11% für einen referenznahen und 1.33% für einen referenzfernen Punkt. Der grösste Fehler bei der Bestimmung von Winkeln war 0.7°. Die vom JAWS-3D gemessenen Geschwindigkeiten bis auf 80 mm/s entsprachen sehr gut den Sollwerten mit einem Durchschnittsfehler von 3 mm/s. Für höhere Geschwindigkeiten nahm die Ungenauigkeit bis auf 26 mm/s bei 210 mm/s zu.